Dielectric Properties of α-Fe 0

AUTHOR(S):

Iwauchi, Kōzō; Yamamoto, Shigehisa; Bando, Yoshichika; Koizumi, Naokazu

CITATION:

Iwauchi, Kōzō ...[et al]. Dielectric Properties of α-Fe 0. Bulletin of the Institute for Chemical Research, Kyoto University 1970, 48(4-5): 159-170

ISSUE DATE:

1970-12-19

URL:

http://hdl.handle.net/2433/76340

Bull. Inst. Chem. Res., Kyoto Univ., Vol. 48, Nos. 4-5, 1970

Dielectric Properties of α-Fe_2O_3

Kōzō Iwauchi*, Shigehisa Yamamoto**, Yoshichika Bando**
and Naokazu Koizumi*

Received September 9, 1970

Dielectric properties of α-Fe_2O_3 derived from a number of origins were studied in the temperature range from 77°K to 373°K. Dielectric dispersions were observed in α-Fe_2O_3 prepared from electrolytic iron. The structure yielding the dispersion was fairly stable for heat treatment. The mechanism of dispersion was discussed in terms of the interfacial polarization which arised from heterogeneities composed of less-conductive and conductive phases. The latter was caused by traces of ferrous ions formed at high temperatures in the sample of ferric oxide.

INTRODUCTION

In the oxides of iron α-Fe_2O_3 is the most stable compound. For the non-existence of Fe^{++} ions α-Fe_2O_3 has higher electrical resistivity than other oxides of iron such as Fe_3O_4, FeO, and ferrites. It has been reported, however, that at the temperature above 1200°C there is the possibility of the appearance of Fe^{++} ions in α-Fe_2O_3.[1] When the oxides contain ferrous ions, the hopping of electrons between ferrous and ferric ions gives rise to higher conductivity. Thus for samples possessing both the conductive and less-conductive phases the Maxwell-Wagner interfacial polarizations [2,3] are observed. With the surface modified by the use of mild reducing condition of sintering Hirbon reported the interfacial polarization in the sintered compacts of α-Fe_2O_3.[4] On the other hand, in α-Fe_2O_3 containing other ions of different valencies such as Ti^{+4} ions polarizations due to permanent dipoles of Fe^{++}—Fe^{+++} induced by Ti^{+4} ions were observed at very low temperature.[5]

In this work, dielectric dispersions on a variety of α-Fe_2O_3 prepared with various methods were measured in the wide temperature range. In α-Fe_2O_3 with impurity ions such as Ti^{+4} or Zn^{+2} interfacial polarizations were observed. Moreover, strange to say, in the α-Fe_2O_3 prepared from high purity electrolytic iron remarkable inter facial polarizations were always found. The origin of these polarizations is discussed in viewpoint of impurities and ferrous ions.

EXPERIMENTAL PROCEDURE

The samples of α-Fe_2O_3 were prepared for the study of dielectric properties from four different series of origins given in Table I.

* 岩内幸蔵，小泉直一: Laboratory of Dielectrics, Institute for Chemical Research, Kyoto University, Uji, Kyoto.
** 山本恵久，坂東尚周: Laboratory of Crystal and Powder Chemistry, Institute for Chemical Research, Kyoto University, Uji, Kyoto.

Table I. Methods of Preparing Samples of α-Fe_2O_3.

Origin	Method, Added solution	Precipitation	Heat treatment	Product
1. $Fe(NO_3)_3$	aq. NaOH	α-Fe_2O_3	600～1000°C	α-Fe_2O_3
2. $FeSO_4 \cdot 7H_2O$	decomposition at 700°C	α-Fe_2O_3	1000～1200°C	α-Fe_2O_3
	aq. NaOH	α-FeOOH	1000°C	α-Fe_2O_3
	aq. NaOH	γ-FeOOH	1000°C	α-Fe_2O_3
	aq. $H_2C_2O_4$	$FeC_2O_4 \cdot 2H_2O$	1000°C	α-Fe_2O_3
—half and half	aq. H_2SO_4, $H_2C_2O_4$	$FeC_2O_4 \cdot 2H_2O$	1000°C	α-Fe_2O_3
	aq. H_2SO_4, NH_4OH	p.p.t	1000°C	α-Fe_2O_3
3. Fe	aq. H_2SO_4, $H_2C_2O_4$	$FeC_2O_4 \cdot 2H_2O$	1000°C	α-Fe_2O_3*
(electrolytic	aq. H_2SO_4, NH_4OH	p.p.t	1000°C	α-Fe_2O_3*
iron)	aq. HCl, HNO_3	$Fe(NO_3)_3$	1000°C	α-Fe_2O_3*
	aq. H_2SO_4	α-FeOOH	700°C	α-Fe_2O_3
	aq. H_2SO_4	α-FeOOH	800°C	α-Fe_2O_3*
	aq. H_2SO_4	α-FeOOH	1000°C	α-Fe_2O_3*
	aq. H_2SO_4	α-FeOOH	1000°C in O_2 (1 atm)	α-Fe_2O_3*
	aq. H_2SO_4	α-FeOOH	1000°C pulverization	α-Fe_2O_3*
	aq. H_2SO_4	α-FeOOH	1000→800°C anneal	α-Fe_2O_3*
	aq. H_2SO_4	γ-FeOOH	1000°C	α-Fe_2O_3*
4. Fe	aq. H_2SO_4, $H_2C_2O_4$	$FeC_2O_4 \cdot 2H_2O$	1000°C	α-Fe_2O_3*
(metal)	aq. H_2SO_4, NH_4OH	p.p.t	1000°C	α-Fe_2O_3*

Heat treatment was carried out in air unless otherwise specified.

* The sample showing such a type of dispersion as given in Fig. 7.

Series 1.

Ferric nitrate used as starting material is the commercial reagent. Precipitates of α-Fe_2O_3 were obtained by hydrolysis of ferric nitrates at 80°C. These particles are very fine ($\sim$0.1 μ) as shown in Fig. 1.

Series 2.

Ferrous sulfate used as starting material is the commercial reagents. Particles of α-Fe_2O_3 were obtained by decomposition of $FeSO_4 \cdot 7H_2O$, α-FeOOH, γ-FeOOH and $FeC_2O_4 \cdot 2H_2O$

Series 3.

Electrolytic iron used as starting material was obtained from Showa Denko Co. which was the highest purity iron metal commercially available. To obtain high purity α-Fe_2O_3 particles, α-FeOOH was calcined in air at 600°C (Fig. 2) and 1000°C (Fig. 3). In this case α-FeOOH was precipitated from dilute H_2SO_4 solution containing electrolytic iron powder by bubbling the air through it. Crystals of α-FeOOH were plate like with the dimension of 1～2 $\mu \times 500$ A $\times$ 200 A.

On the other hand, impurity ions such as Ti^{+4}, Zn^{+2}, $Mn^{+2\sim+4}$, Ni^{+2} and Cu^{+2} were added to α-Fe_2O_3 samples in series 2 and 3. Impurity doped α-Fe_2O_3 was

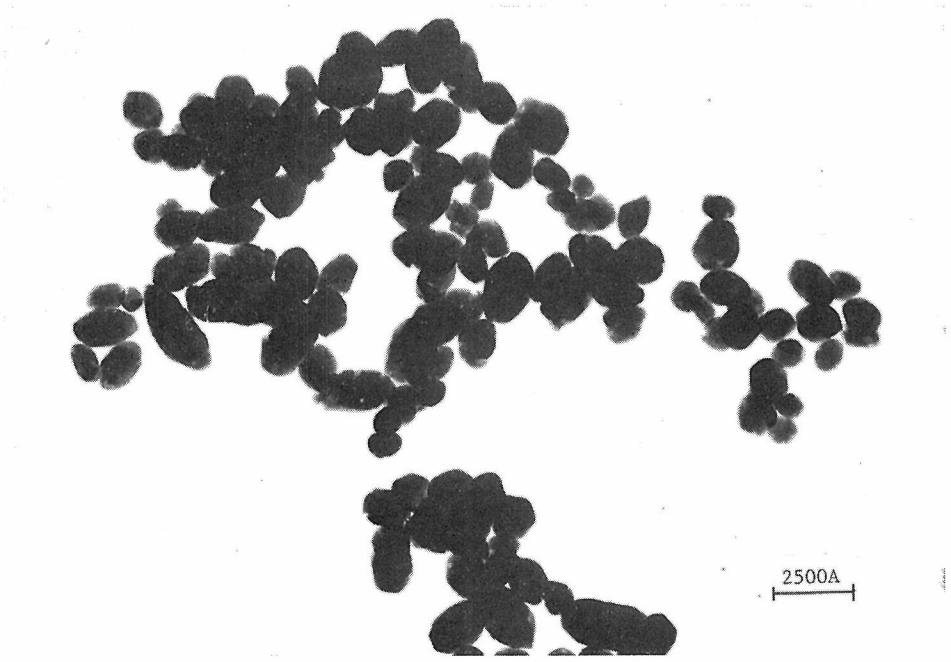

Fig. 1. Electron micrograph of α-Fe_2O_3 obtained as precipitates from aqueous solution.

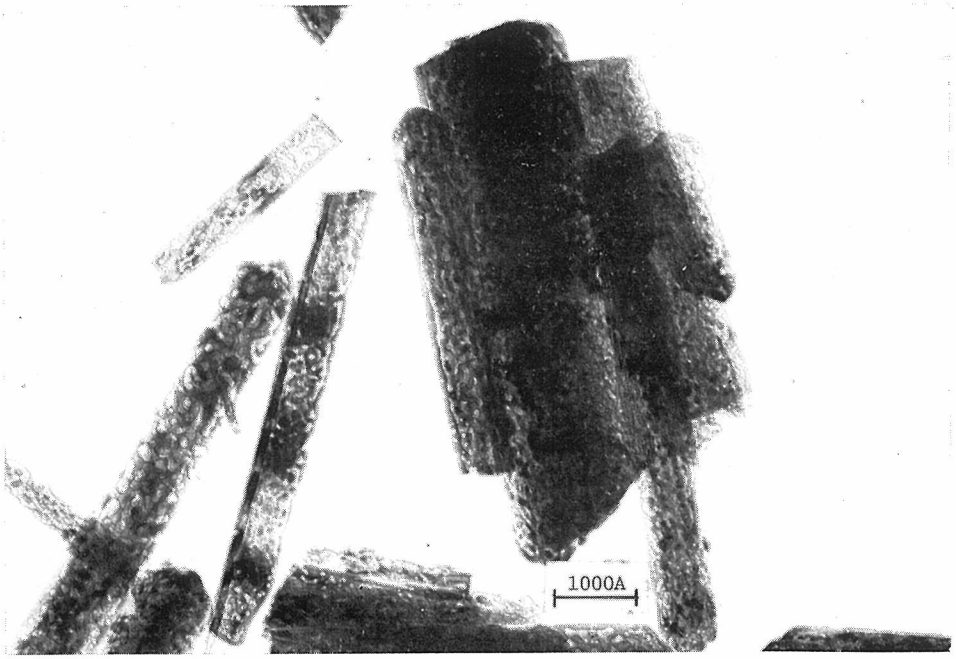

Fig. 2. Electron micrograph of α-Fe_2O_3 particles prepared by calcination of α-FeOOH at 600°C for one hour.

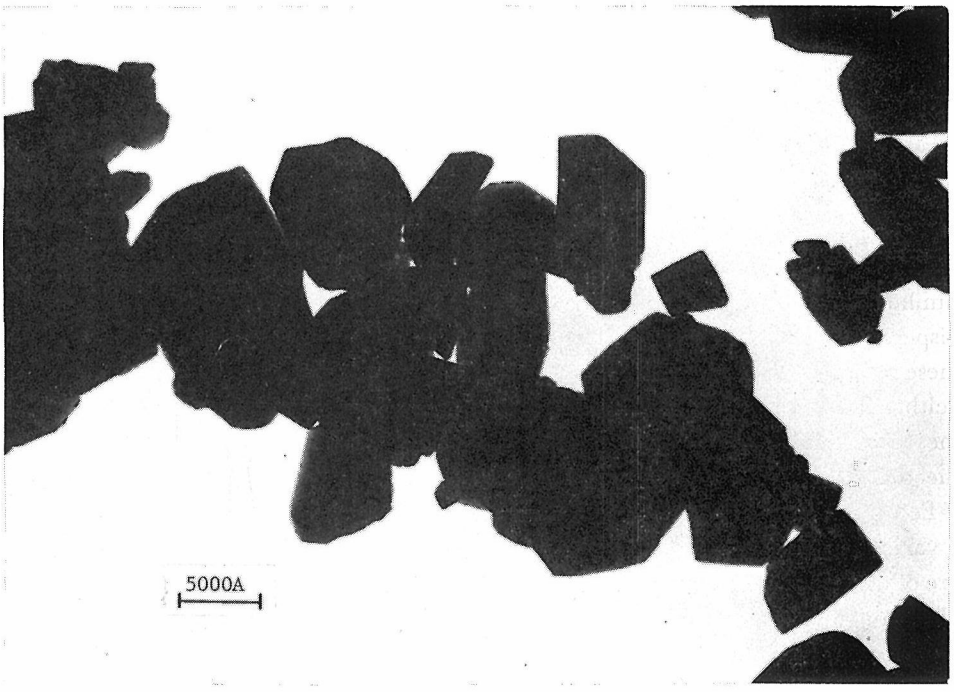

Fig. 3. Electron micrograph of α-Fe_2O_3particles prepared by calcination of α-FeOOH at 1000°C for 5 hours.

made by the calcination of precipitations which were obtained from ferrous sulfate mixed with the sulfate of each impurity ion.

The special type of dielectric cell in which powders were compressed under the pressure of 1500 kg/cm^2 was set in vacuum of $10^{-3}\sim10^{-4}$ mmHg for one day in order to remove the influence of adsorbed water. After removal of the adsorbed water the dielectric measurements were started. An Ando TR-IB transformer bridge and selective amplifires were used for the dielectric measurements. Dielectric dispersions and their temperature dependences were measured in the temperature range from 77°K to 373°K, over the frequency range from 20 Hz to 1 MHz. At low temperatures the cell was filled with dry nitrogen gas to cool the samples rapidly. Since the dielectric diepersions were little influenced with the change of compression pressure employed in this work, it was considered that the contact resistance between particles plays no essential role in the experiment.

RESULTS

1. Dielectric properties of α-Fe_2O_3 in series 1 and 2

All dielectric constants, losses and conductivities in this paper are apparent ones for the powder samples which contain the vacant spaces.

Typical frequency dependence of dielectric constant of α-Fe_2O_3 is shown in Fig. 4 which is the data of fine α-Fe_2O_3 particles (series 1) prepared from aqueous solution of ferric salt $Fe(NO_3)_3$. All α-Fe_2O_3 samples of series 1 and 2 in Table I gave the

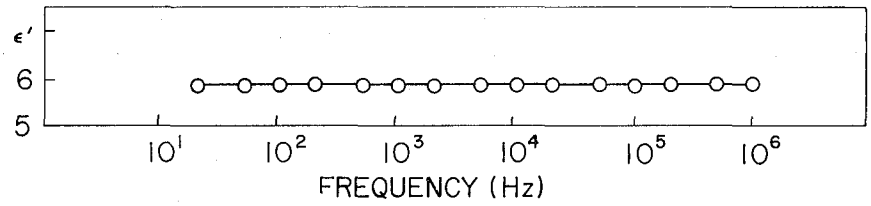

Fig. 4. Frequency dependence of dielectric constant of α-Fe_2O_3 prepared from the origin of series 1 or 2 at −160°C.

similar frequency dependences and dielectric constants. These samples exhibit no dispersion in the temperature range from 77°K to 373°K as shown in Fig. 4. From these results of dielectric measurements it is clear that these α-Fe_2O_3 samples have neither dipoles producing the Debye type dispersions nor heterogeneities yielding the Maxwell-Wagner type dispersions but are composed of the uniform structure of the oxide. Hence the dielectric constant shown in Fig. 4 is an intrinsic value of α-Fe_2O_3 powders. The values of dielectric constants of α-Fe_2O_3 in the series 1 and 2 varies within about 10 percent with the methods of preparation. These variations are of no importance considering the variation of vacant spaces in the powder samples. Near room temperature the dielectric constants at lower frequencies become remarkably large by the effects of traces of adsorbed water, ions, and defects.

2. Dielectric properties of α-Fe_2O_3 in series 3 and 4

Figure 5 shows the dielectric dispersion of α-Fe_2O_3 prepared from α-FeOOH

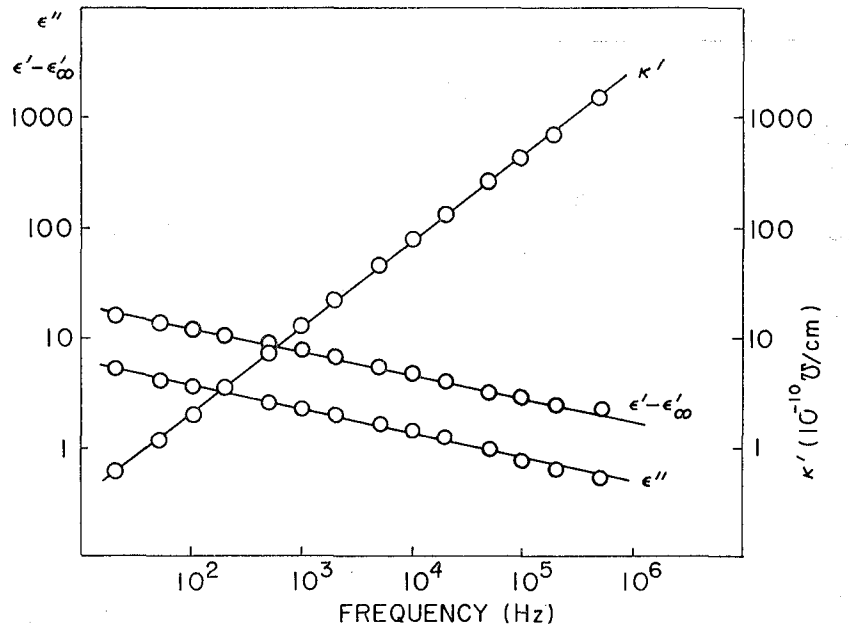

Fig. 5. Frequency dependence of dielectric constant and loss of α-Fe_2O_3 particles at room temperature which were obtained by calcination of α-FeOOH at 1000°C for 5 hours and annealed at 800°C for 24 hours.

in series 3 measured at room temperature. Figure 6 is the complex plane plots of Fig. 5. This type of frequency dependence is called the wedge type dispersion[7] which represents the above mentioned increase of dielectric constant at lower frequencies. However, at low temperature this sample of α-Fe_2O_3 shows the remarkable dispersion given in Figs. 7 and 8. Temperature dependences of dielectric constant and loss are given in Figs. 9 and 10 respectively. From these figures it is seen that

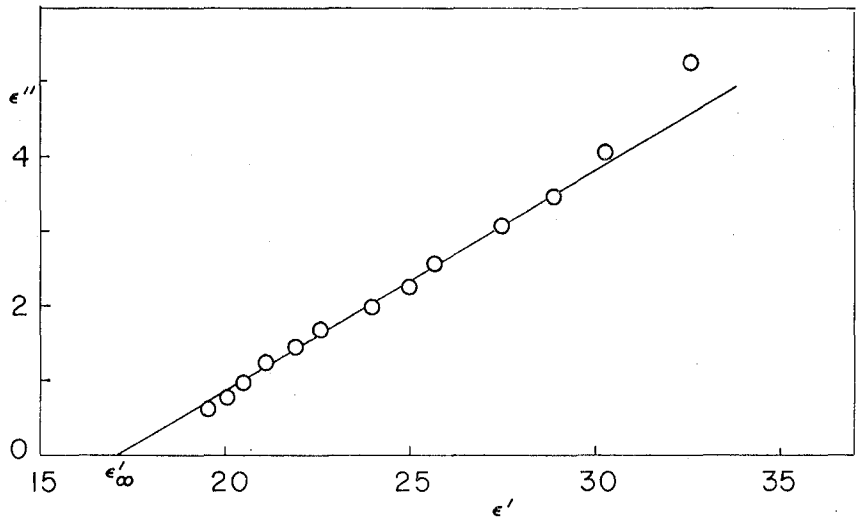

Fig. 6. Complex plane plots of Fig. 5

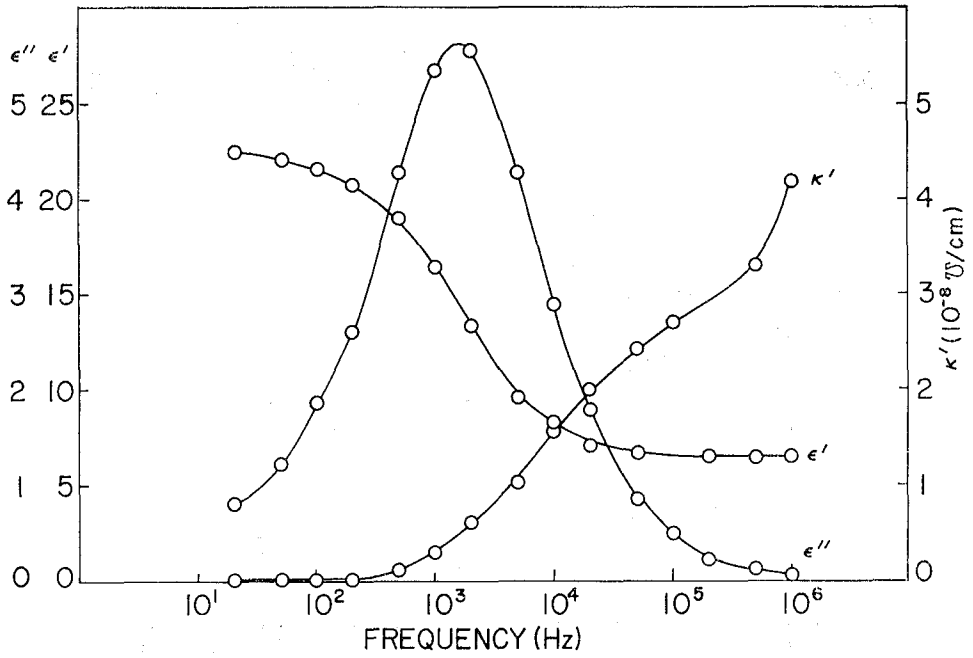

Fig. 7. Dielectric dispersion of α-Fe_2O_3 particles shown in Fig. 5 measured at −147°C.

there exists either permanent dipoles or heterogeneities in samples. If one compares these figures with that of the sample of series 1, there is a great difference in the frequency dependence. It is noteworthy that α-Fe_2O_3 derived from high purity material (electrolytic iron) has a more complicated structure which shows such dielectric dispersion as in Fig. 7 than that from the samples in series 1 and 2. The sample showing this remarkable dispersion is prepared by the calcination of α-FeOOH in series 3 at 1000°C and annealed at 800°C for 24 hours. For further heat treatments this structure was very stable and never disappeared. The appearance of the structure was not influenced by the pressure of oxygen in the calcination. In the sample prepared by the calcination of α-FeOOH below 800°C such structure was not observed but only in the sample prepared above 800°C. The dispersion was not specific in α-Fe_2O_3 from α-FeOOH in siries 3 but was found in α-Fe_2O_3 from other compounds in series 3. On the other hand, in the samples of series 1 and 2 no such types of

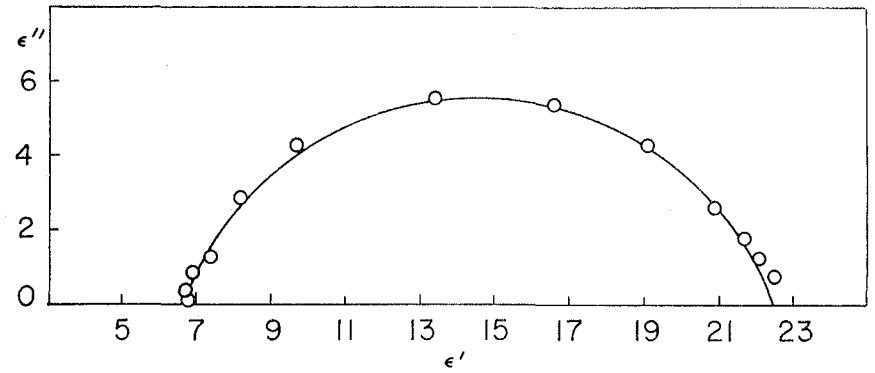

Fig. 8. Complex plane plots of the dispersion given in Fig. 7.

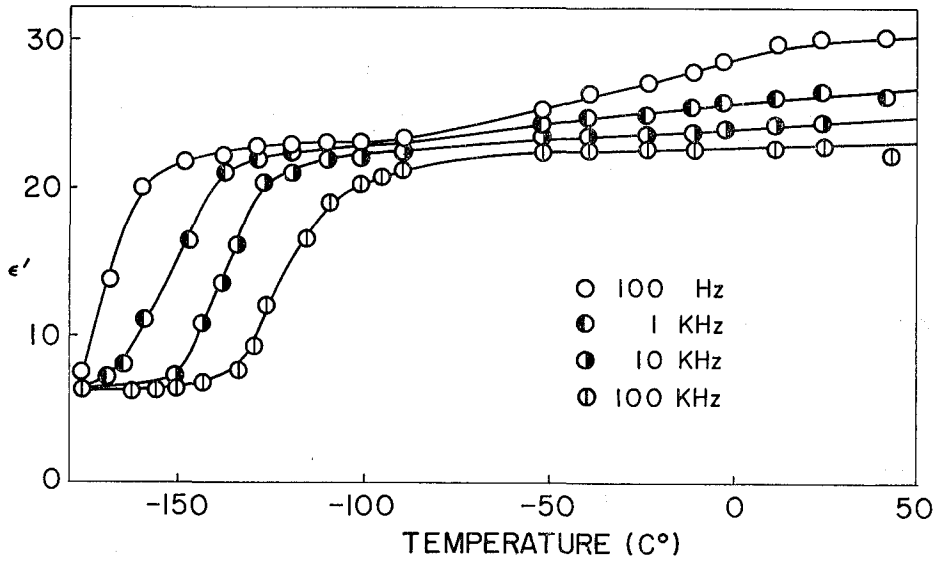

Fig. 9. Temperature dependence of dielectric constant of the α-Fe_2O_3 sample shown in Fig. 5.

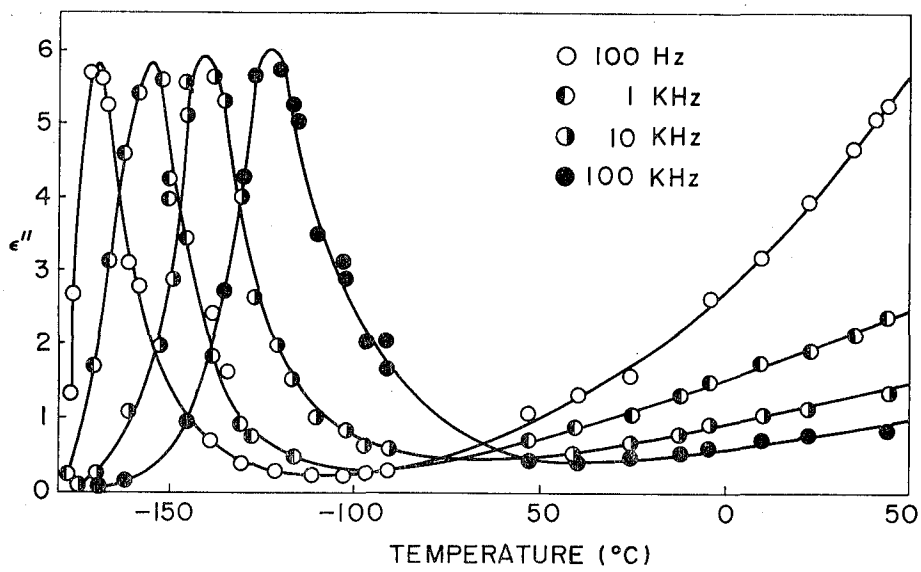

Fig. 10. Temperature dependence of dielectric loss of the sample shown in Fig. 5.

dispersions as in Fig. 7 took place. Hence it was found that there was distinct difference between these two types of samples as given in Table I. In series 3 the temperature at which the dispersion was observed varied with the method of preparation of α-Fe_2O_3 samples although in the α-Fe_2O_3 samples prepared from α-FeOOH it was almost the same (−147°C) for any heat treatment shown in Table I. In the case of pure iron metal from other origin (series 4) the same sort dielectric dispersion was also observed.

3. Impurity effects

Figure 11 and 12 show complex plane plots of the dielectric dispersion of α-Fe_2O_3 obtained by the calcination of $FeC_2H_2O_4 \cdot 2H_2O$ or $Fe(OH)_2$ precipitated

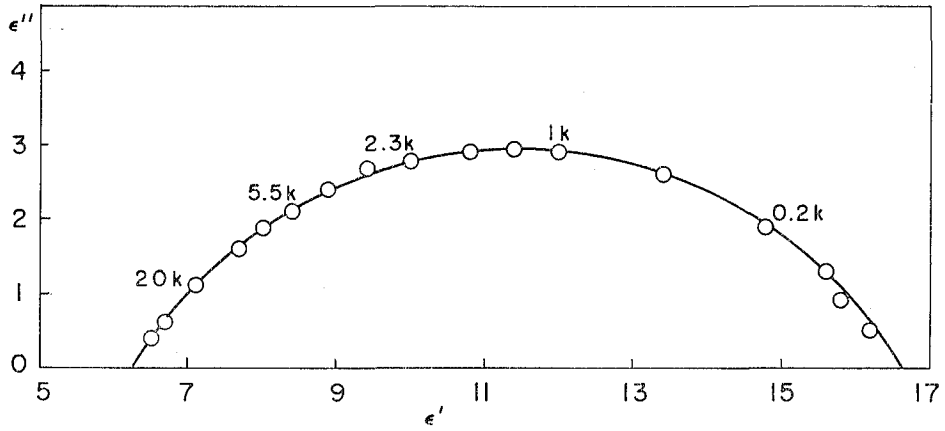

Fig. 11. Complex plane plots of the dielectric dispersion of α-Fe_2O_3 containing 5% Zn ions at −135°C.

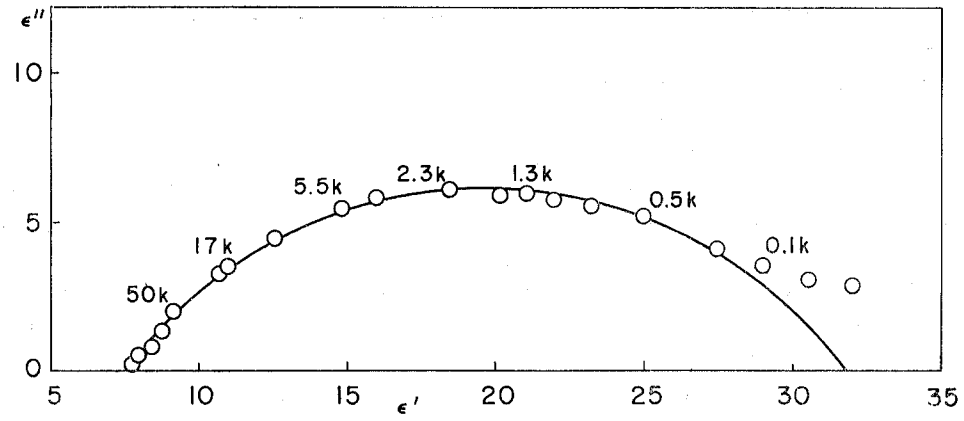

Fig. 12. Complex plane plots of the dielectric dispersion of α-Fe_2O_3 containing 0.1% Ti ions at −135°C.

from $FeSO_4$ solution in series 2 containg Ti and Zn ions respectively. These dispersions were caused by the impurity ions (Ti^{+4}, Zn^{+2}). On the other hand, Mn, Ni, and Cu ions did not produce such a dispersion. Far from that, when Mn ions were added to the α-Fe_2O_3 sample in series 3, the sample did not show the dispersion such as that of pure α-Fe_2O_3 in series 3. It appeared that there are complicated effects of impurity ions upon the dielectric properties of α-Fe_2O_3.

DISCUSSION

The dispersion shown in Fig. 7 was characteristic in α-Fe_2O_3 of series 3 since it was very stable as mentioned in the previous section and there was clear distinction of property among series of samples listed in Table I. The limiting value of dielectric constant at higher frequencies, ε_h, in this dispersion is the same one (the intrinsic value of α-Fe_2O_3 powder) as in Fig. 4 for the samples of series 1 and 2. The limitting value of dielectric constant at lower frequencies ε_l, in Fig. 7 is about 22.5, being exceedingly higher compared with those of the samples of series 1 and 2. This is considered to be caused by the non-intrinsic structure of the α-Fe_2O_3 sample. As the non-intrinsic structure of the α-Fe_2O_3 sample either existence of permanent dipoles or heterogeneity of electrical property in the sample considered. Although there have been reports which insist on the existence of permanent dipoles in α-Fe_2O_3 containing Ti^{+4} ions,[5] Fe_3O_4-γFe_2O_3,[8] and alkali halide,[9,10] it would be plausible to consider the existence of such heterogeneity as produces the Maxwell–Wagner type dispersion rather than to consider the existence of dipoles in pure α-Fe_2O_3. This is supported by the fact that in the samples of series 3 relaxation frequency and temperature for the dispersion were different from sample to sample while the group of samples prepared from α-FeOOH showed the almost same relaxation frequencies. Moreover, from the result that the dispersion was observed only in the samples prepared above 800°C it seemed that the structure of the oxide produced at high temperature was responsible for the dispersion.

For the interfacial polarization there must be at least two kinds of phases in the sample of α-Fe_2O_3. Differences of dielectric constants of these types of oxides are too small to support the existence of the two phases in α-Fe_2O_3. Only small local deviations from stoichiometry, however, might be the reason for the large differences of electrical resistivities which can easily give rise to the above mentioned two phases in the oxides and such deviations will probably not affect the dielectric constant. Of course no trace of second phase could be detected in α-Fe_2O_3 samples by x-ray diffraction.

Since α-Fe_2O_3 possesses extremely lower electrical conductivity, it is difficult to expect any less conductive oxides containing other metal ions in the samples of α-Fe_2O_3. Therefore, it is necessary to consider the existence of the part of more conductive oxide in the α-Fe_2O_3 sample. Because the α-Fe_2O_3 samples showing such types of dispersions as in Fig. 7 are derived from electrolytic iron which possesses the highest purity commercially available, the origin of the conductive oxides in α-Fe_2O_3 will be ferrous ions produced in α-Fe_2O_3 rather than impurity ions which can make conductive ferrites.

Table II shows the dependence of two limitting dielectric constants, ε_l and ε_h on the temperature of calcination. According to the Maxwell-Wagner[2,3] theory it is seen that ε_l depends on the fraction of the conductive layer. Then the result in this table that ε_l becomes larger with increasing the temperature of calcination may suggests that the fraction of conductive layers, namely an amount of ferrous ions increase with increasing the temperature of calcination. This is consistent with the fact that the higher the temperature, the more stable the ferrous ions become. Therefore it is considered that conductive layers are composed of ferrous ions.

Table II. Dependence of Dielectric Constant of α-Fe_2O_3 Prepared from α-FeOOH in no. 3 Series upon the Temperature of Calcination in Air.

Methods of calcination		Dielectric constant	
Firing	Cooling	ε_l*	ε_h*
1200°C 2hr	rapid	27.5	6
1000°C 5hr	slow	26	6
1000°C 5hr → 800°C 24hr	slow	22.5	6
800°C 5hr	slow	17	6
1000°C 5hr → 700°C 48hr	slow	14.7	7.15
1000°C 5hr → 400°C 48hr	slow	24	6
700°C 6hr	slow	6	6
1000°C 5hr → 700°C 48hr → 1000°C 5hr	slow	19.3	6.6

* ε_l and ε_h are the limitting values of dielectric constant at lower and higher frequencies respectively.

Table III. The Results of Analisis of Some Samples Selected as Representatives of Each Series in Table 1 by an Atomic Absorption Spectro-photometry.

Samples		Impurities (%)						
		Na	Ni	Cu	Co	Zn	Mn	Mg
Fe	(no. 3)	0.0037	0.00285	0.0016	0.0724	0.0076	0.0030	0.00016
α-FeOOH	(no. 3)	0.0015	0.0105	0.0019	0.0137	0.0113	0.0011	0.00009
α-Fe_2O_3	(no. 3)	0.0023	0.0105	0.0018	0.0252	0.0300	0.0011	0.00013
$FeSO_4 \cdot 7H_2O$	(no. 2)	0.0016	0.0067	0.0009	0.0125	0.0011	0.0074	0.00028
α-Fe_2O_3	(no. 2)	0.0126	0.0224	0.0022	0.0254	0.0034	0.0244	0.00044

Since no dispersion was observed in the sample of α-Fe_2O_3 derived from $FeSO_4$ solution composed of series 2 and 3 origins in half, it is seen that a very small amount of impurity ions in series 2 samples prevents the appearance of the dispersion shown in Fig. 7, that is, the appearance of Fe^{+2} ions in α-Fe_2O_3, because the sample composed of both series 2 and 3 origins should show such type of dispersion if a very small amount of impurity ions in series 3 samples is responsible for the dispersion. Table III shows the comparison of the result of analysis by an atomic absorption spectro-photometry between these two series of α-Fe_2O_3 samples. The samples of the upper three rows belong to series 3 and those of lower two rows to series 2. Though from this table it can not be seen definitely which samples are purer it is noteworthy that Mn ions are more abundant in the samples of series 1 and 2 than in the samples of series 3. In fact the sample of series 3 added especially with 0.02% Mn ions shows no such dispersion as in Fig. 7. It may be supposed that traces of Mn ions present in α-Fe_2O_3 prevent the appearance of ferrous ion in α-Fe_2O_3.

On the other hand, the samples of series 2 added with small amount of Ti and Zn impurity ions gave the dispersion. While the presence of Zn ions (for instance 0.02%) was not effective, in the case of Ti 0.02% ions in α-Fe_2O_3 were enough to produce the dispersion. Although the result that a very small amount of Ti ions in α-Fe_2O_3 is effective in the formation of the dispersion seems to suggest the existence of the permanent dipoles of Fe^{++}-Fe^{+++} induced by Ti^{+4} ions in α-Fe_2O_3, from the results throughout this work the heterogeneity model would be chosen, namely there are both conductive part containing Fe^{++} ions and less-conductive part composed of only ferric oxide in α-Fe_2O_3.

REFERENCES

(1) P. M. Hansen, Constitution of Binary Alloys, McGraw Hill Book Company New York, (1958) 688.

(2) J. C. Maxwell, Electricity and Magnetism, Oxford University Press, London (1873), vol. 1, Sec. 328.

(3) K. W. Wagner, *Ann. Physik*, **40**, 817 (1913); *Arch Electroch.* **2,** 371 (1914).

(4) R. B. Hirborn, *J. Appl. Phys.* **36,** 1553 (1965).

(5) J. Volger, *Philips tech. Rdsch.* **22**, 306 (1960/61).

(6) T. Takada *et al.*, *Bull. Inst. Chem. Res. Kyoto University*, **43,** 406 (1965).

(7) N. Koizumi and T. Hanai, *Bull. Inst. Chem. Res. Kyoto University*, **42,** 115 (1964).

(8) O. Jantzen, *Z. Angew. Phys.* **18,** 560 (1965).
(9) R. G. Brekenridge, Imperfections in Nearly Perfect Crystals, John Wiley & Sons, Inc., New York, (1952).
(10) D. Grissom and W. H. Hartwig, *J. Appl. Phys.* **37,** 4784 (1966).